Journal of Metals, Materials and Minerals, Vol. 31, No. 2, pp. 71-77, 2021

The enhancement of ethanol gas sensors response based on calcium and zinc co-doped $LaFeO_3/Fe_2O_3$ thick film ceramics utilizing yarosite minerals extraction as Fe_2O_3 precursor

Endi SUHENDI[1,*], Zeany Luckyta AMANDA[1], Muhamad Taufik ULHAKIM[1], Andhy SETIAWAN[1], and Dani Gustaman SYARIF[2]

[1] *Program Studi Fisika, Universitas Pendidikan Indonesia, Jl. Dr. Setiabudi No. 229, Bandung, 40154, Indonesia*
[2] *Pusat Sains dan Teknologi Nuklir Terapan, Badan Tenaga Nuklir Nasional, Jl. Tamansari No. 71, Bandung, Indonesia*

***Corresponding author e-mail:** endis@upi.edu

Received date:
21 January 2021
Revised date
2 April 2021
Accepted date:
30 April 2021

Keywords:
Co-doped $LaFeO_3/Fe_2O_3$;
$LaFeO_3/Fe_2O_3$ thick film ceramics;
Yarosite mineral;
Ethanol gas sensing

Abstract

A gas sensor is a renewed interest of research which has been developed to make a device that can be detected the harmful gases and applied in the several fields of industries. In this paper, we report the modified of gas sensor based thick film ceramic $LaFeO_3/Fe_2O_3$ by added calcium and zinc co-doping prepared by screen-printed technique. In this work, yarosite mineral was utilized as Fe_2O_3 precursor. It aims to take the advantages of abundance natural resources in Indonesia to save a cost in gas sensor fabrication. Then, x-ray diffraction (XRD), scanning electron microscopy (SEM) and electrical properties characterization were applied to the calcium and zinc co-doped $LaFeO_3/Fe_2O_3$-based thick film ceramics. It is obtained that the crystal structures were cubic with crystallite size at about 51.19 nm and 48.17 nm. SEM images informed that calcium and zinc co-doped caused the larger pores of $LaFeO_3/Fe_2O_3$. It indicates that the gas sensors shows a response to the ethanol gases. Lastly, calcium and zinc co-doped can be a potential candidate to enhance the highly performance of gas sensors. Moreover, yarosite mineral also can be used to develop the future perspectives of ethanol gas sensors.

1. Introduction

In recent decades, gas sensors have become an interesting topic in the research community. It is focused on modified materials as though added doping which aims to develop the gas sensors with good performances. Currently, gas sensors based on metal-oxide semiconductor (MOS) also have been attracting attention to study, especially to monitor the health and safety processes due to their advantages such as low-cost, easy in implementation and high compatibility [1]. MOS that were widely used as gas sensors were ZnO [2], SnO_2 [3], Fe_2O_3 [4], In_2O_3 [5], WO_3 [6], and $LaFeO_3$ [7]. Up to now, MOS-based gas sensors were classified into two groups i.e. n-type and p-type [8]. These types of MOS gas sensors were known based on the resistance changes on the gas exposed. The n-type of MOS gas sensors shows the reducing resistance while gases were exposed and its contrarily for p-type of MOS gas sensors [9]. N-type of MOS gas sensors have limitations in performance and p-type of MOS gas sensors appear as alternative materials to be applied as gas sensors [10]. MOS gas sensors have the advantages of being able to detect the harmful gases with a highly response [11], such as on detecting methanol [12], acetone [13], formaldehyde [14], toluene [15], acetylene [16], benzene [17], and ethanol [18].

Ethanol has the promising potential and can be used in several fields such as pharmaceutical, traffic safety on transportations and food industry [19]. It is important to utilize the gas sensor to detect ethanol gases for the safety and untoward incident in the industrial processes. Furthermore, the ethanol gas sensors are highly needed and very important in many conditions such as avoiding the driver who drunk in the driving condition and so on [20]. Therefore, the development of MOS gas sensor to detect the ethanol gases were necessary. One of the materials that were widely used as ethanol gas sensors is $LaFeO_3$ [21-24]. It due to a good response from $LaFeO_3$ in the field of gas sensors [25]. $LaFeO_3$ were synthesized from $LaCl_3.7H_2O$ and Fe_2O_3 [26]. Fe_2O_3 can be obtained from the raw material as though of yarosite minerals. In the recent years, studied about raw materials especially in utilization of yarosite minerals as Fe_2O_3 precursor has been doing by Aliah *et al.* [27]. Moreover, the ulitization of yarosite minerals as Fe_2O_3 precursor also as the alternative solution to saving a cost. Yarosite minerals have the higher contains of Fe_2O_3 up to 91.30% and the 8.7% others were impurities as shown in Table 1 [26].

Aliah *et al*. (2019) claimed that yarosite minerals have a good potential to applied in many sectors, either gas sensors [27]. In the gas sensor application, response is the most important parameter that needs to be considered. Many researchers modified the materials with added doping to enhance the response of the gas sensor as doing by Liu *et al.* [28], Kou *et al.* [29] and Singh *et al*. [30]. Thereout, some researchers have been developed a gas sensors with added doping especially for $LaFeO_3$. It has been done by Ariyani *et al.* [26] and Suhendi *et al*. [31]. Ariyani (2018) developed $LaFeO_3$ with added CaO as a doping while Suhendi (2019) added Al_2O_3 as a doping. Their research also utilized

Table 1. Impurities contains of yarosite minerals.

No.	Compound	Weight%
1	Fe_2O_3	91.30
2	Al_2O_3	3.30
3	SiO_2	2.05
4	TiO_2	3.02
5	CaO	0.16
6	MnO	0.17

the yarosite minerals for Fe_2O_3 precursor. The response of the ethanol gas sensor that occurs in their experiment also indicates that yarosite mineral can used as material sensing. Then, the added a doping to the main materials were aim to prevent the growth of crystallite size. It caused the reduce of crystallite size and become smaller [23,25]. The smaller crystallite size of materials shows a better response as gas sensors [32].

Based on the explained above, we report the ethanol gas sensor fabrication based on calcium and zinc co-doping $LaFeO_3/Fe_2O_3$. Fe_2O_3 precursor originated from the yarosite mineral which is abundant in Indonesia. The utilization of yarosite minerals will save a cost in gas sensors fabricated. Moreover, the co-doping was added to find out the influence of co-doping to the morphological and response of gas sensors to the ethanol gases.

2. Experimental

2.1 Chemicals

In this works, the main chemicals that prepared were lanthanum(III) chloride heptahydrate ($LaCl_3.7H_2O$), yarosite minerals extraction as Fe_2O_3 precursor, calcium oxide (CaO), zinc oxide (ZnO) and ammonium hydroxide (NH_2OH) 25 M. Then, the chemicals that used as solvent were hydrochloric acid (HCl) 2 M and aquadest. Furthermore, the other chemicals were prepared to fabricate the thick films i.e. silver (Ag) paste as electrodes, ethyl cellulose and alpha-terpineol.

2.2 Synthesis of calcium and zinc co-doped $LaFeO_3/Fe_2O_3$ powder

Calcium and zinc co-doped $LaFeO_3/Fe_2O_3$ powder were prepared by coprecipitation method in accordance with the experiment that has been done by Suhendi *et al.* [33] in 2019. To prepare calcium and zinc co-doped $LaFeO_3/Fe_2O_3$ powder, 0.5 mol $LaCl_3.7H_2O$ was initially dissolved in 20 mL aquadest. Then, 0.44 mol Fe_2O_3 from yarosite minerals extraction, 0.05 mol CaO and 0.01 mol ZnO were dissolved in 20 mL HCl 5 M, respectively. Furthermore, all solutions were mixed under vigorous stirring using a magnetic stirrer until homogeneous. The homogeneous solution was subsequently added by NH_2OH 25 M in slowly until the pH of the solution was about 7 and leave it in overnight. Then, the resulting precipitate was filtered, dried at 100°C for 8 h and calcined at 800°C for 2 h. Similar synthesis procedures were used to produce $LaFeO_3/Fe_2O_3$ powder as comparison using 0.5 mol $LaCl_3.7H_2O$ and 0.5 mol Fe_2O_3.

2.3 Thick film fabrication and characterization

The experimental steps to produce a thick film were divided into three steps. The initial step was preparing the material paste based calcium and zinc co-doped $LaFeO_3/Fe_2O_3$. To prepare the material paste, organic vehicles were made from ethyl cellulose and alpha-terpineol in ratio 1:9. The organic vehicles were mixed with calcium and zinc co-doped $LaFeO_3/Fe_2O_3$ powder and stirrer until homogeneous. The second step was preparing the substrate, the alumina substrate which has the thickness of 0.5 mm and the size of 1 cm × 0.5 cm was coated with silver (Ag) electrode and its preparation using screen-printing technique as shown in Figure 1. Then, the substrate was fired at 600°C for 10 min. The last step, material paste based calcium and zinc co-doped $LaFeO_3/Fe_2O_3$ was coated over the silver (Ag) electrode using screen-printing technique as shown in Figure 2 and fired at 600°C for 2 h.

Calcium and zinc co-doped $LaFeO_3/Fe_2O_3$-based thick film ceramics which have been made were characterized by x-ray diffraction (XRD) and scanning electron microscopy (SEM) to observe the crystal and morphological structures, respectively. XRD characterization also informed the lattice parameters and crystallite size which were calculated using the Debye-Scherrer formula as shown in Equation (1) [34-37]. SEM characterization was conducted by taking up the images of the calcium and zinc $LaFeO_3/Fe_2O_3$ surface to analyze the morphological structures.

$$D = \frac{K\lambda}{\beta \cos\theta} \quad (1)$$

where D is the crystallite size (nm), K is the Scherrer constant which has the value in the range of 0.9 to 1.0 [38], this works were used $K = 0.9$ accordance to Moshi *et al.* (2012) statement that normally scherrer constant was taken is 0.9 [39], λ is the x-ray wavelength (1.5406 Å), β is the full width at half maximum (FWHM) and θ is the angle of the Bragg diffraction.

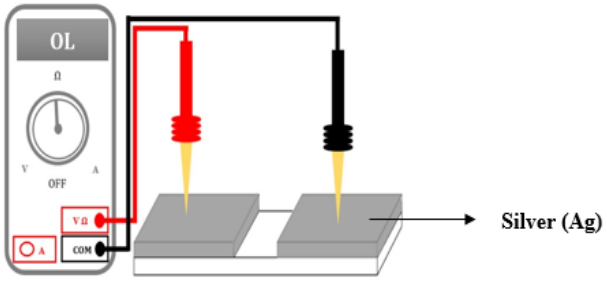

Figure 1. Silver (Ag) coated on the alumina substrate.

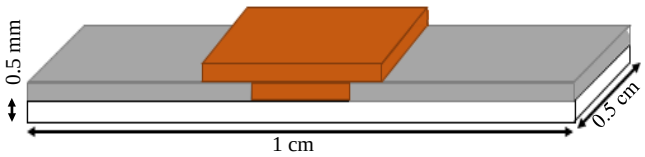

Figure 2. Illustration of thick film ceramics that were made in this work.

Furthermore, the electrical properties characterization was conducted using gas chamber tools to observe the performance of calcium and zinc co-doped $LaFeO_3/Fe_2O_3$ on detect the ethanol gases. The electrical properties informed the resistance function of temperature (R-T) which recorded every 5°C increase. These measurement processes were shown in Figure 3. These R-T functions were analyzed to determine the response of the samples on detecting the ethanol gases which were calculated using Equation (2) [40-42]. In this work, the various concentrations of ethanol gases were treated to the samples i.e. 100, 200, and 300 ppm.

$$Response = \frac{R_g - R_a}{R_a} \quad (2)$$

where R_g is the resistance of the samples in the gas chamber tools with ethanol gases containing and R_a is the resistance of the samples in the ambient conditions (without ethanol gases).

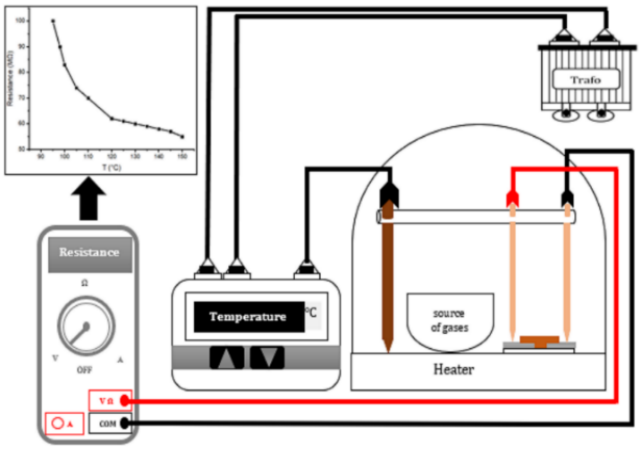

Figure 3. Illustration of electrical properties measurements for ethanol gas sensor based on calsium and zinc co-doped $LaFeO_3/Fe_2O_3$ or their comparison ($LaFeO_3/Fe_2O_3$).

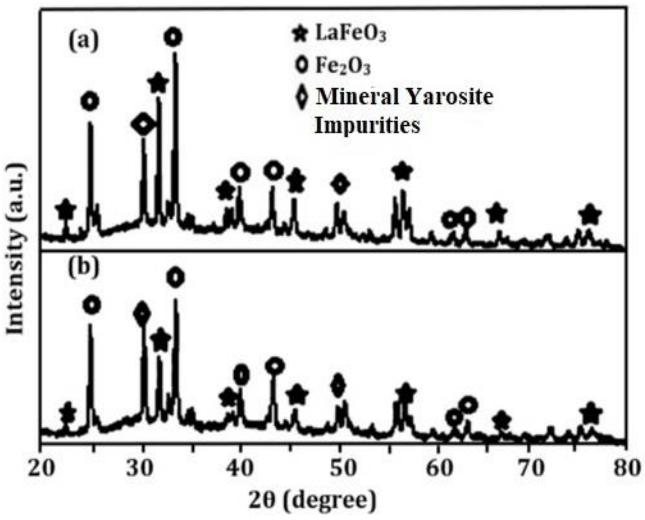

Figure 4. XRD pattern of thick film ceramics based (a) $LaFeO_3/Fe_2O_3$ (b) calcium and zinc co-doped $LaFeO_3/Fe_2O_3$.

3. Results and discussion

To examine the characteristics of calcium and zinc co-doped $LaFeO_3/Fe_2O_3$-based thick film ceramics, the $LaFeO_3/Fe_2O_3$ were made as comparison. The characteristics were characterized using XRD and obtained the results as shown in Figure 4. The patterns exhibit well reflections at 2θ = 22.55°, 32.17°, 39.68°, 46.11°, 57.46°, 67.43° and 76.74° corresponding to JCPDS No. 96-154-2033 which shows cubic structures. The reflections were matched with (100), (110), (111), (200), (211), (220), and (301) of $LaFeO_3$. Then, the average of crystallite size was calculated using the Debye-Scherrer equation as mentioned in Equation (1). The calculation found that calcium and zinc decreased the crystallite size, 51.19 nm to 48.17 nm. It occurs because the substituting calcium and zinc as co-doping on $LaFeO_3/Fe_2O_3$ prevent the growth of crystallite size. It is caused by Ca^{2+} (0.134 nm) that has a smaller ionic radius than La^{3+} (0.136 nm) [43]. It is also obtained on Zn^{2+} (0.064 nm) to Fe^{3+} (0.074 nm) [44]. The XRD characterization also reports that calcium and zinc co-doped caused the lattice parameter of $LaFeO_3/Fe_2O_3$ to sustain an expansion of about 3.8977 Å to 3.9516 Å. The expansion was obtained due to elastic deformation in the material which caused the strain when the dopan were added [45].

Other characterization was also explored to examine the characteristics of calcium and zinc co-doped $LaFeO_3/Fe_2O_3$. SEM characterization was conducted to investigate the characteristics of calcium and zinc co-doped $LaFeO_3/Fe_2O_3$. The SEM images were shown in Figure 5. It is found that calcium and zinc co-doping caused the pores of $LaFeO_3$/ Fe_2O_3 became larger. It gives a better response of gas sensors [46]. It is indicated that calcium and zinc co-doping increased the response of $LaFeO_3/Fe_2O_3$ based gas sensor to the ethanol gases.

The response of calcium and zinc co-doped $LaFeO_3/Fe_2O_3$ to ethanol gases was informed by resistance function of temperature that obtained from resistance measurement in the electrical properties characterization as shown in Figure 6. The resistances were reduced as increasing temperature at any concentration of ethanol gases. The lowered resistance indicated that the conductivity of the gas sensors were increasing. This phenomenon is due to the electron transfer which increases the hole of the material to equate the Fermi level [47].

Figure 7 shows the response of calcium and zinc co-doping $LaFeO_3$/ Fe_2O_3 and their comparison ($LaFeO_3/Fe_2O_3$) to the ethanol gases. The responses were derived from R-T graphical, then processed using Equation (2). The result informed that the calcium and zinc co-doping increased the response of $LaFeO_3/Fe_2O_3$ as shown in Table 2. The optimal response was subject to 300 ppm of ethanol gas exposed based on calcium and zinc co-doping $LaFeO_3/Fe_2O_3$. Moreover, these co-doping also reduce the operating temperature, namely 205°C to 190°C.

This experiment was utilized the yarosite mineral as Fe_2O_3 precursor. Table 1 indicates that yarosite mineral can be utilized as ethanol gas sensor material in the future. This experiment gives a better response than previously studies which utilized yarosite mineral as doing by Suhendi *et al.* [33] and Aliah *et al.* [48]. It is obtained by the co-doping which play an important role in the gas sensor performance

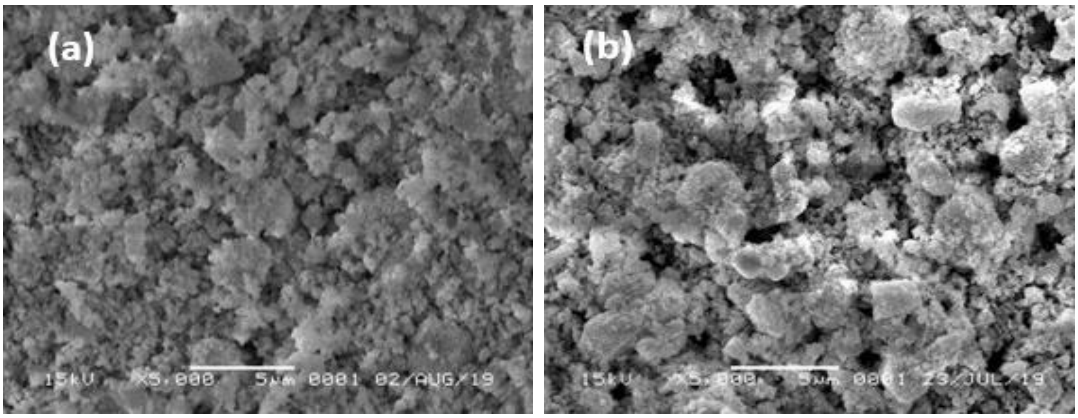

Figure 5. SEM images of thick film ceramics based (a) $LaFeO_3/Fe_2O_3$ (b) calcium and zinc co-doped $LaFeO_3/Fe_2O_3$.

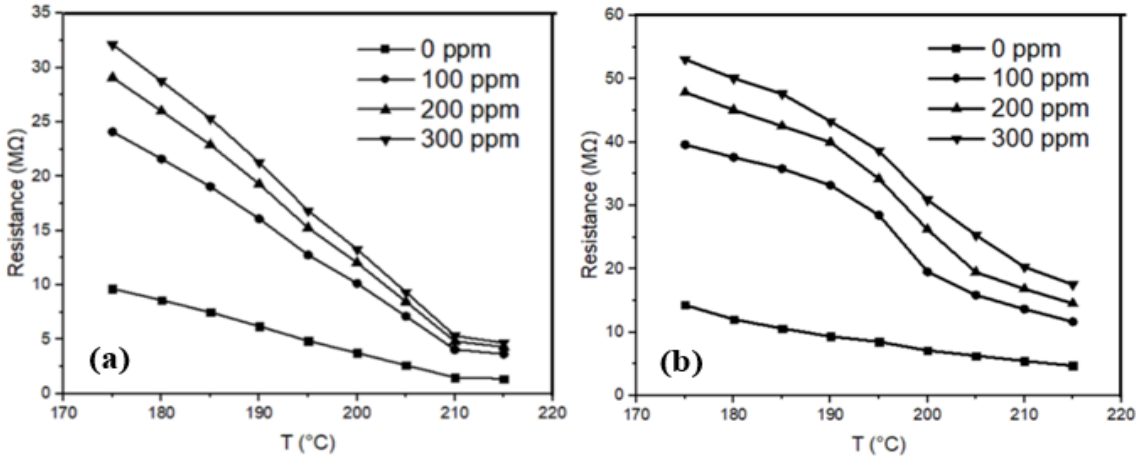

Figure 6. Resistance changes at different temperature in the ambient condition (0 ppm) and ethanol exposed (100 ppm, 200 ppm, 300 ppm) of thick film ceramics based on (a) $LaFeO_3/Fe_2O_3$ (b) calcium and zinc co-doped $LaFeO_3/Fe_2O_3$.

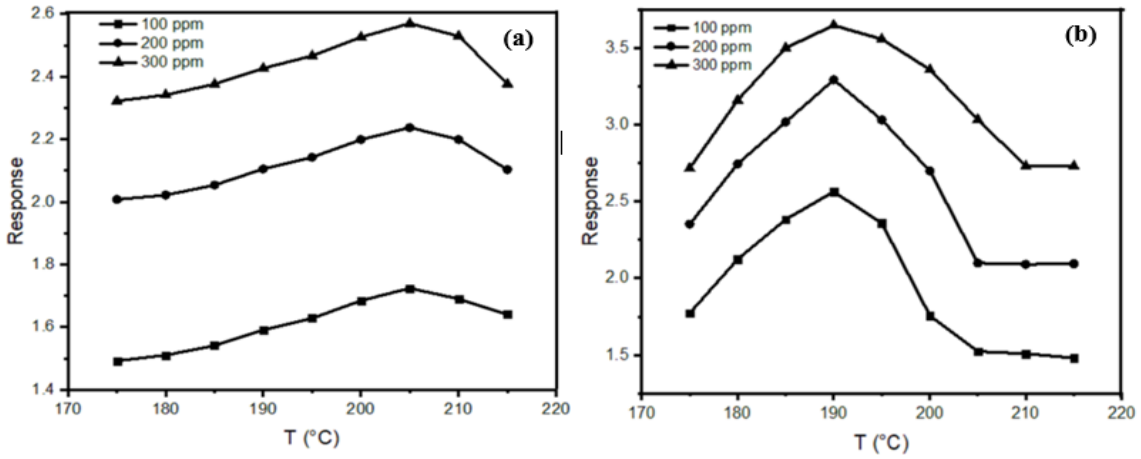

Figure 7. Response of thick film ceramics based on (a) $LaFeO_3/Fe_2O_3$ (b) calcium and zinc co-doped $LaFeO_3/Fe_2O_3$ to ethanol gases.

Table 2. The response of calcium and zinc co-doped $LaFeO_3/Fe_2O_3$ with their comparison ($LaFeO_3/Fe_2O_3$).

Materials	Response of ethanol gas sensor in various concentration			Ref.
	100 ppm	200 ppm	300 ppm	
$LaFeO_3/Fe_2O_3$	1.724	2.237	2.569	This work
Calcium and zinc co-doped $LaFeO_3/Fe_2O_3$	2.563	3.292	3.645	This work
$LaFeO_3$ doping SrO	1.900	2.860	3.050	[33]
$ZnFe_2O_4/Mn_2O_3$	~0.59	~0.63	~0.76	[48]

The responses occur by explaining the sensing mechanism. The mechanism of MOS sensor were explained by chemical reaction as shown in Equation (3) and (4) below [22]:

$$C_2H_5OH + 60^{n-}_{(ads)} \rightarrow 2CO_2 + 3H_2O + 6ne^- \quad (3)$$

$$C_2H_5OH + 60^{n-}_{(native)} \rightarrow 2CO_2 + 3H_2O + 6ne^- \quad (4)$$

These equations informed that the surface of the material, in this work based on calcium and zinc co-doped $LaFeO_3/Fe_2O_3$ will produce more holes with increasing temperature and concentration of ethanol gas. It is due to the electron on the material becoming more energetic to jump from the valence band to the conduction band. This phenomenon obtained the increase of hole production and it occurs until the sensor element is heated to a certain temperature. Afterward, the hole production will be decreased caused by the hole which combines with O^- and O^2 ions and reform O^2 [49]. A certain temperature becomes an operating temperature of the gas sensing that was fabricated.

4. Conclusions

In summary, calcium and zinc co-doped $LaFeO_3/Fe_2O_3$ were made using coprecipitation method, then prepared by screen-printed technique to be a thick film ceramic that applied as ethanol gas sensors. These materials were characterized by XRD, SEM and electrical properties. These materials have a large pore and it causes a response to ethanol gases. The experiment confirmed that the crystal structure of $LaFeO_3/Fe_2O_3$ were cubic. Calcium and zinc co-doping decreased the $LaFeO_3/Fe_2O_3$ crystallite size of about 51.19 nm to 48.17 nm. Calcium and zinc co-doped also decreased the operating temperature of gas sensor based $LaFeO_3/Fe_2O_3$, it was 205℃ to 190℃. The response also increased as the concentration of ethanol gases increased. Lastly, this work informed that calcium and zinc can be a good material doping to enhanced the gas sensor response, especially to ethanol gases. Moreover, in the future perspective, the utilized yarosite mineral also can be used to save a cost in the gas sensor fabrication.

Acknowledgements

This work was financially supported by "Hibah Penelitian Dasar Unggulan Perguruan Tinggi" Kementerian Riset, Teknologi dan Pendidikan Tinggi Republik Indonesia Research Grants in the fiscal year 2020.

References

[1] S. Zhao, Y. Shen, X. Yan, P. Zhou, Y. Yin, R. Lu, C. Han, B. Cui, and D. Wei, "Complex-surfactant-assisted hydrothermal synthesis of one-dimensional ZnO nanorods for high-performance ethanol gas sensor," *Sensor and Actuator B: Chemical*, vol. 286, pp. 501-511, 2019.

[2] J. Wang, S. Fan, Y. Xia, C. Yang, and S. Komarneni, "Room-temperature gas sensors based on ZnO nanorod/Au hybrids: visible-light-modulated dual selectivity to NO_2 and NH_3," *Journal of Hazardous Materials*, vol. 381, pp. 120919, 2020.

[3] J. Hu, M. Chen, Q. Rong, Y. Zhang, H. Wang, D. Zhang, X. Zhao, S. Zhou, B. Zi, J. Zhao, J. Zhang, Z. Zhu, and Q. Liu, "Formaldehyde sensing performance of reduced graphene oxide-wrapped hollow SnO_2 nanospheres composites," *Sensors and Actuators B: Chemical*, vol. 307, pp. 127584, 2020.

[4] A. Umar, A. A. Ibrahim, R. Kumar, H. Albargi, M. A. Alsaiari, and F. Ahmed, "Cubic shaped hematite (α-Fe_2O_3) microstructures composed of stacked nanosheets for rapid ethanol sensor application," *Sensors and Actuators B: Chemical*, vol. 326, pp. 128851, 2020.

[5] W. Qin, Z. Yuan, H. Gao, and F. Meng, "Ethanol sensors based on porous In_2O_3 nanosheet-assembled micro-flowers," *Sensors*, vol. 20(1-14), pp. 3353, 2020.

[6] B. Bouchikhi, T. Chludzinski, T. Saidi, J. Smulko, N. E. Bari, H. Wen, and R. Lonescu, "Formaldehyde detection with chemical gas sensors based on WO_3 nanowires decorated with metal nanoparticles under dark condition and UV light irradiation," *Sensors and Actuators B: Chemical*, vol. 320, pp. 128331, 2020.

[7] B. Wang, Q. Yu, S. Zhang, T. Wang, P. Sun, X. Chuai, and G. Lu, "Gas sensing with yolk-shell $LaFeO_3$ microspheres prepared by facile hydrothermal synthesis," *Sensors and Actuators B: Chemical*, vol. 258, pp. 1215-1222, 2018.

[8] C. Liu, H. Lu, J. Zhang, Z. Yang, G. Zhu, F. Yin, J. Gao, C. Chen, and X. Xin, "Abnormal p-type sensing response of TiO_2 nanosheets with exposed {001} facets," *Journal of Alloys and Compounds*, vol. 705, pp. 112-117, 2017.

[9] S. M. Majhi, G. K. Naik, H. Lee, H. Song, C. Lee, I. Lee, and Y. Yu, "Au@NiO core-shell nanoparticles as a p-type gas sensor: novel synthesis, characterization, and their gas sensing properties with sensing mechanism," *Sensors and Actuators B: Chemical*, vol. 268, pp. 223-231, 2018.

[10] P. Hao, G. Qiu, P. Song, Z. Yang, and Q. Wang, "Contruction of porous $LaFeO_3$ microspheres decorated with NiO nanosheets for high response ethanol gas sensors," *Applied Surface Science*, vol. 515, pp. 146025, 2020.

[11] K. S. Choi, S. Park, and S. Chang, "Enhanced ethanol sensing properties based on SnO_2 nanowires coated with Fe_2O_3 nanoparticles," *Sensors and Actuators B: Chemical*, vol. 238, pp. 871-879, 2017.

[12] Y. Li, D. Deng, X. Xing, N. Chen, X. Liu, X. Xiao, and Y. Wang, "A high performance methanol gas sensor based on palladium-platinum-In_2O_3 composited nanocrystalline SnO_2," *Sensors and Actuators B: Chemical*, vol. 237, pp. 133-141, 2016.

[13] S. Liang, J. Li, F. Wang, J. Qin, X. Lai, and X. Jiang, "Highly sensitive acetone gas sensor based on ultrafine α-Fe_2O_3 nanoparticles," *Sensors and Actuators B: Chemical*, vol. 238, pp. 923-927, 2017.

[14] D. Meng, D. liu, G. Wang, Y. Shen, X. San, M. Li, and F. Meng, "Low-temperature formaldehyde gas sensors based on NiO-SnO_2 heterojunction microflowers assembled by thin porous nanosheets," *Sensors and Actuators B: Chemical*, vol. 273, pp. 418-428, 2018.

[15] H. Gao, L. Zhao, L. Wang, P. sun, H. Lu, F. Liu, X. Chuai, and G. Lu, "Ultrasensitive and low detection limit of toluene gas sensor based on SnO_2-decorated NiO nanostructure," *Sensors and Actuators B: Chemical*, vol. 255, pp. 3505-3515, 2018.

[16] M. S. Park, R. Yoo, B. Jang, Y. Park, M. Kim, H. Lee, and W. Lee, "Highly sensitive acetylene sensing properties of aland In-doped Zno quantum dots," *17th International Meeting on Chemical Sensors – IMCS 2018*, pp. 796-797, 2018.

[17] T. Sauerwald, T. Baur, M. Leidinger, W. Reimringer, L. Spinelle, M. Gerboles, G. kok, and A. Schutze, "Highly sensitive benzene detection with metal oxide semiconductor gas sensor – an inter-laboratory comparison," *Journal of Sensors and Sensor Systems*, vol. 7, pp. 235-243, 2018.

[18] Z. Song, J. Zhang, and J. Jiang, "Morphological evolution, luminescence properties and a high-sensitivity ethanol gas sensor based on 3D flower-like MoS_2-ZnO micro/nanosphere arrays," *Ceramics International*, vol. 46, pp. 6634-6640, 2020.

[19] C. Wang, Z. Wang, R. Xi, L. Zhang, S. Zhang, L. Wang, and G. Pan, "In situ synthesis of flower-like ZnO on Gan using electrodeposition and its application as ethanol gas sensor at room temperature," *Sensor and Actuator B: Chemical*, vol. 292, pp. 270-276, 2019.

[20] H. Yu, J. Wang, B. Zheng, B. Zhang, L. Liu, Y. Zhou, C. Zhang, and X. Xue, "Fabrication of single crystalline WO_3 nanobelts based photoelectric gas sensor for detection of high concentration ethanol gas at room temperature," *Sensors and Actuators A: Physical*, vol. 303, pp. 111865, 2020.

[21] Y. Zhang, Z. Duan, H. Zou, and M. Ma, "Fabrication of electrospun $LaFeO_3$ nanotubes via annealing technique for fast ethanol detection," *Meterials Letter*, vol. 215, pp. 58-61, 2018.

[22] E. Cao, Z. Chu, H. Wang, W. Hao, L. Sun, and Y. Zhang, "Effect of film thickness on the electrical and ethanol sensing characteristics of $LaFeO_3$ nanoparticle-based thick film sensors," *Ceramics International*, vol. 44, pp. 7180-7185, 2018.

[23] J. Xiang, X. Chen, X. Zhang, L. Gong, Y. Zhang, and K. Zhang, "Preparation and characterization of Ba-doped $LaFeO_3$ nanofibers by electrospinning and their ethanol sensing properties," *Materials Chemistry and Physics*, vol. 213, pp. 122-129, 2018.

[24] M. Chen, H. Wang, J. Hu, Y. Zhang, K. Li, D. Zhang, S. Zhou, J. Zhang, Z. Zhu, and Q. Liu, "Near-room-temperature ethanol gas sensor based on mesoporous Ag/Zn-$LaFeO_3$ nanocomposite," *Adavanced Materials Interfaces*, vol. 6, pp. 1801453, 2019.

[25] W. Wei, S. Guo, C. Chen, L. Sun, Y. Chen, W. Guo, and S. Ruan, "High sensitive and fast formaldehyde gas sensor based on Ag-doped $LaFeO_3$ nanofibers," *Journal of Alloys and Compounds*, vol. 695, pp. 1122-1127, 2017.

[26] N. I. Ariyani, D. G. Syarif, and E. Suhendi, "Fabrication and characterization of thick film ceramics $La_{0.9}Ca_{0.1}FeO_3$ for ethanol gas sensor using extraction of Fe_2O_3 from yarosite minerals", IOP Conf. Ser.: Mater. science. eng. 384 012037.

[27] H. Aliah, D. G. Syarif, R. N. Iman, A. Sawitri, W. Darmalaksana, A. Setiawan, A. Malik, and P. Gumarang, "Structure analysis of nanocomposites ZnO:Fe_2O_3 based mineral yarosite as Fe_2O_3 source and its application probability," Materialstoday: Proceedings, vol. 13, pp. 36-40. 2019.

[28] X. Liu, L. Jiang, X. Jiang, X. Tian, X. Sun, Y. Wang, W. He, P. Hou, X. Deng, and X. Xu, "Synthesis of Ce-doped In_2O_3 nanostructures for gas sensors applications," *Applied Surface Sciences*, vol. 428, pp. 478- 484, 2018.

[29] X. Kou, N. Xie, F. Chen, T. Wang, L. Guo, C. Wang, Q. Wang, J. Ma, Y. Sun, H. Zhang, and G. Lu, "Superior acetone gas sensor based on electrospun SnO_2 nanofibers by Rh doping," *Sensors and Actuators B: Chemical*, vol. 256, pp. 861-869, 2018.

[30] G. Singh, Virpal, and R. C. Singh, "Highly sensitive gas sensor based on Er-doped SnO_2 nanostructures and its temperature dependent selectivity towards hydrogen and ethanol," *Sensors and Actuator B: Chemical*, vol. 282, pp. 373-383, 2019.

[31] E. Suhendi, N. A. Lidiawati, D. G. Syarif, and A. Setiawan, "Synthesis and characterization of Al_2O_3-doped $LaFeO_3$ thick film ceramics for ethanol gas sensing application," *Oriental Journal of Chemistry*, vol. 35, pp. 283-288, 2019.

[32] M. A. M. Akhir, S. A. Rezan, K. Mohamed, M. M. Arafat, A. S. M. A. Haseeb, and H. L. Lee, "Synthesis of SnO_2 nanoparticles via hydrothermal method and their gas sensing applications for ethylene detection," *Materialstoday: Proceedings*, vol. 17, pp. 810-819, 2019.

[33] E. Suhendi, M. T. Ulhakim, A. Setiawan, and D.G. Syarif, "The effect of SrO doping on $LaFeO_3$ using yarosite extraction based ethanol gas sensors performance fabricated by coprecipitation method," *International Journal of Nanoelectronics and Materials*, vol. 12, pp. 185-192, 2019.

[34] D. Zhang, J. Liu, C. Jiang, P. Li, and Y. Sun, "High-performance sulfure dioxide sensing properties of layer-by-layer self-assembled titania-modified graphene hybrid nanocomposite," *Sensors and Actuators B: Chemical*, vol. 245, pp. 560-567, 2017.

[35] A. Beniwal, P. K. Sahu, and S. Sharma, "Sol-gel spin coating assited room temperature operated nanostructured ZnO ethanol sensor with behavior transformation," *Journal of Sol-Gel Science and Technology*, vol. 88, pp. 322-333, 2018.

[36] L. Song, L. Yang, Z. Wang, D. Liu, L. Luo, X. Zhu, Y. Xi, Z. Yang, N. Han, F. Wang, and Y. Chen, "One-step electrospun SnO_2/MO_x heterostructured nanomaterials for highly selective gas sensor array integration," *Sensor and Actuators B: Chemical*, vol. 283, pp. 793-801, 2019.

[37] L. Lv, P. Cheng, Y. Wang, L. Xu, B. Zhang, C. Lv, J. Ma, and Y. Zhang, "Sb-doped three-dimensional $ZnFe_2O_4$ macroporous spheres for N-butanol chemiresistive gas sensors," *Sensor and Actuators B: Chemical*, vol. 320, pp. 128384, 2020.

[38] A. M. Awwad, N. M. Salem, M. M. Aqarbeh, and F. M. Abdulaziz, "Green synthesis, characterization of silver sulfide nanoparticles and antibacterial activity evaluation," *Chemistry International*, vol. 6, pp. 42-48, 2020.

[39] A. Monshi, M. R. Foroughi, and M. R. Monshi, "Modified scherrer equation to estimate more accurately nano-crystallite size using XRD," *World Journal of Nano Science and Engineering*, vol. 2, pp. 154-160, 2012.

[40] D. Rathore, S. Mitra, R. Kurchania, and R. K. Pandey, "Physicho-chemical properties of $CuFe_2O_4$ nanoparticles as a gas sensor," *Journal of Materials Science: Materials in Electronics*, vol. 29, pp. 1925-1932, 2018.

[41] M. Deshwal, and A. Arora, "Enhanced acetone detection using Au doped ZnO thin film sensor," *Journal of Materials Science: Materials in Electronics*, vol. 29, pp. 15315-15320, 2018.

[42] C. Rana, S. R. Bera, and S. Saha, "Growth of SnS nanoparticles and its ability as ethanol gas sensor," *Journal of Materials Science: Materials in Electronics*, vol. 30, pp. 2016-2029, 2019.

[43] F. Li, Y. Liu, R. Liu, Z. Sun, D. Zhao, and C. Kou, "Preparation of Ca-doped $LaFeO_3$ nanopowders in a reverse microemulsion and their visible light photocatalytic activity," *Materials Letters*, vol. 64, pp. 223-225, 2010.

[44] T. L. Rao, M. Pradhan, and S. Dash, "Structural, microstructure and impedance spectroscopy analysis of Zn^{2+} doped $LaFeO_3$ nanoparticle," *AIP Conference Proceedings*, vol. 2115, pp. 030089S, 2019.

[45] S. A. Kumar, P. Kuppusami, S. Amirthapandian, and Y. Fu, "Effect of Sm co-doping on structural, mechanical and electrical properties of Gd doped ceria solid electrolytes for intermediate temperatur solid oxide fuel cells," *International Journal of Hydrogen Energy*, vol. 45, pp. 29690-29704, 2020.

[46] C. Feng, S. Ruan, J. Li, B. Zou, J. Luo, W. Chen, W. Dong, and F. Wu, "Ethanol sensing properties of $LaCo_xFe_{1-x}O_3$ nanoparticles: Effects of calcination temperature, Co-doping, and carbon nanotube-treatment," *Sensors and Actuators B: Chemical*, vol. 155, pp. 232-238, 2011.

[47] L. Guo, X. Kou, M. Ding, C. Wang, L. Dong, H. Zhang, C. Feng, Y. Sun, Y. Gao, P. Sun, and G. Lu, "Reduce graphene oxide/ α-Fe_2O_3 composite nanofibers for application in gas sensors," *Sensors and Actuators B: Chemical*, vol. 244, pp. 233242, 2017.

[48] H. Aliah, R. N. Iman, A. Sawitri, D. G. Syarif, A. Setiawan, W. Darmalaksana, and A. Malik, "The optimization of $ZnFe_2O_4$/ Mn_2O_3-based nanocomposite ceramic fabrication utilizing local minerals as an ethanol gas detector," *Materials Research Express*, vol. 6, pp. 095908, 2019.

[49] G. F. Fine, L. M. Cavanagh, A. Afonja, and R. Binions, "Metal-oxide semiconductor gas sensors in environmental monitoring," *Sensors*, vol. 10, pp. 5469-5502, 2010.